

Chapter 5

Neural Network Modeling of an Acetylene Hydrogenation System

In this chapter, the front-end acetylene hydrogenation system is utilized to demonstrate the capabilities of the multilayer feedforward networks to model the complex nonlinear system. Section 5.1 briefs about the acetylene and its effects in ethylene manufacturing. Section 5.2 discusses about the ethylene manufacturing licensed of Stone and Webster. Section 5.3 explains the acetylene hydrogenation system categorized into front-end and tailed type. A review of research works studied on such system is provided in section 5.4. The applications of the networks to model the front-end type system are illustrated in section 5.5 and the results and discussions are given in the last section.

5.1 Introduction

Acetylene is a minor product produced from thermal cracking of paraffinic feedstocks. It is an undesirable impurity in polymer-grade ethylene. By the nature of its volatility relative to ethylene, the acetylene stays close to the ethylene-ethane fraction of the cracked gas throughout the fractionation section of an ethylene plant. It is a harmful contaminant in polymer-grade ethylene. Nevertheless, acetylene must be removed prior to the final fractionation of the ethylene from the ethane in order to produce polymer-grade ethylene. The specification of acetylene in ethylene product is now commonly set at 1 ppmv or less.

5.2 Ethylene Manufacturing

To produce polymer-grade ethylene and propylene by thermally cracking paraffinic feedstocks (ethane through hydrocracked residue). Two main process technologies (Stone and Webster Engineering Corp.) are used:

1. USC (ultra selective cracking) – Pyrolysis and quench systems
2. ARS (advanced recovery system) – Cold fractionation.

Designs have been incorporated to meet environmental restrictions.

Process Description: Feeds are sent to USC cracking furnaces (1). Contaminant removal may be installed upstream. Cracking heat may be supplied by gas turbine exhaust. Pyrolysis occurs under the temperature-time control specific to the feedstock and product requirements. Rapid quenching preserves high-olefin yield and generates high-pressure waste heat steam. Lower temperature waste heat is recovered in the downstream quench oil and quench water towers (2). Pyrolysis fuel oil and gasoline distillate are fractionated. Cracked gas (C_4 and lighter) is then compressed (3), scrubbed with caustic to remove acid gases and dried prior to fractionation.

ARS minimizes refrigeration energy by using the techniques of dephlegmator gas chilling (exclusive arrangement with Air Products) and distributed distillation. C_2 and lighter component as well as C_4 and heavier components are separated in the low fouling front-end dual pressure depropanizer (4). Overhead vapor is hydrogenated to remove acetylene (5) and is routed to the ARS (6), where two C_2 streams of varying composition are produced. Hydrogen and methane are separated overhead.

The heavier C_2 stream is deethanized (7) and C_2 overhead passes to the ethylene-ethane fractionator (9). Polymer-grade ethylene product is sent overhead from the ethylene-ethane fractionator.

C_3 s are combined and hydrogenated to remove methyl acetylene and propadiene (10). Polymer or chemical-grade propylene is then produced overhead from the C_3 superfractionator (11).

C₄ and heavier coproducts are further separated in a sequence of distillation steps. Ethane and propane are typically recycle cracked. Refrigeration is supplied by cascade ethylene/propylene systems.

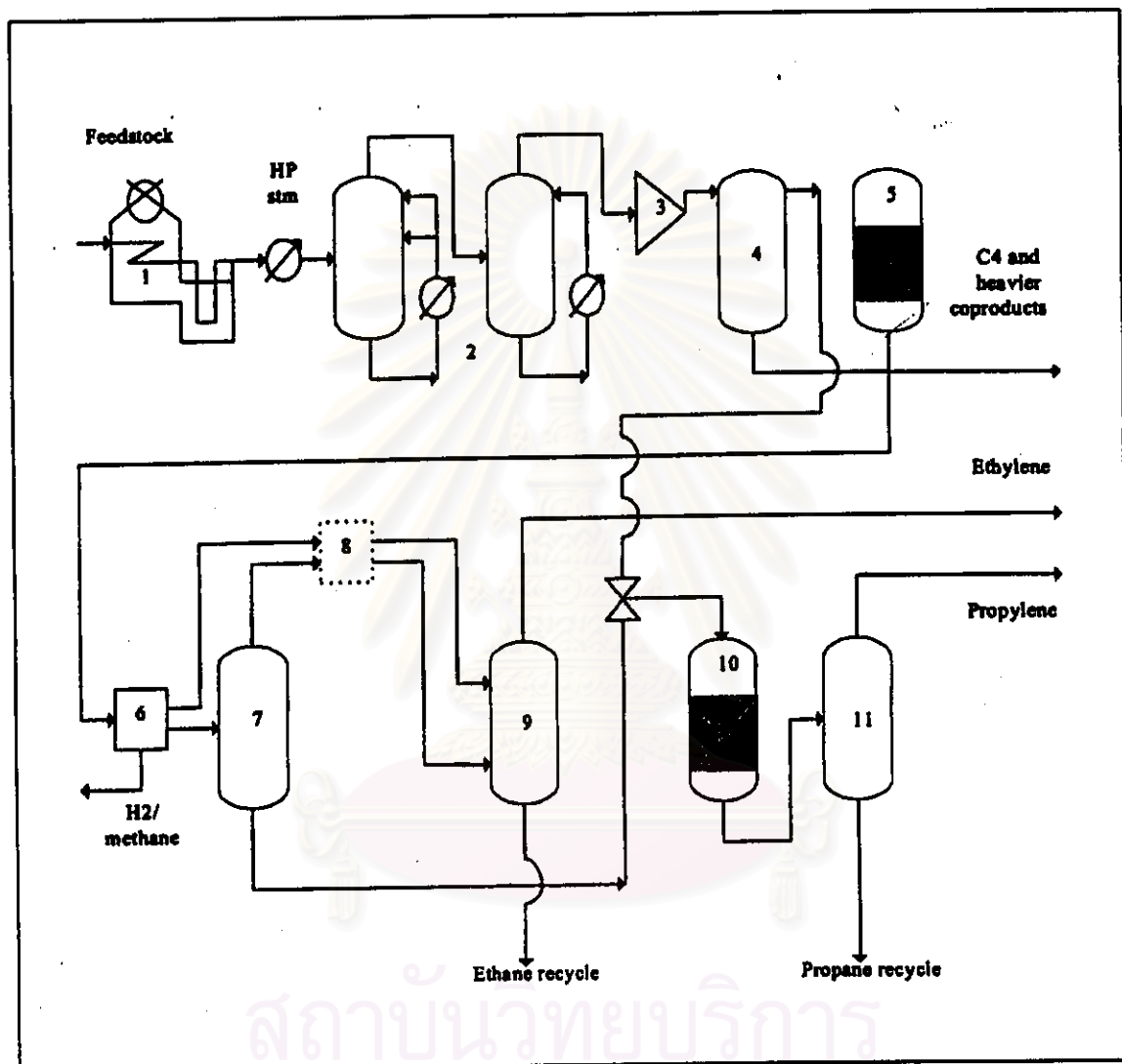


Figure 5.1: Ethylene plant diagram with front-end acetylene hydrogenation system.

Specific advantages of ARS technology are: 1. Reduced chilling train refrigeration load in the dephlegmator, 2. Simultaneous chilling/prefractionation in the dephlegmator, 3. Reduced methane content in feed to demethanizer, 4. Deethanizer bypassing, 5. Dual feed ethylene fractionator (lower reflux ratio) and 6. resulting refrigeration demand reduction (approx. 75%).

Economics: Ethylene yields range from 57% (ethane, high conversion) to 28% (heavy hydrogenated gas oils). Corresponding specific energy consumption range from 3,000 kcal/kg to 6,000 kcal/kg

5.3 Types of Acetylene Hydrogenation Systems

Acetylene hydrogenation systems are usually located at two different places in the purification section of the ethylene plant (Lam and Lloyd, 1972; Derrien, 1986).

According to its location, the acetylene hydrogenation system can be classified into two schemes. One is a front-end design, the other is a tail-end design as described in the following subsection.

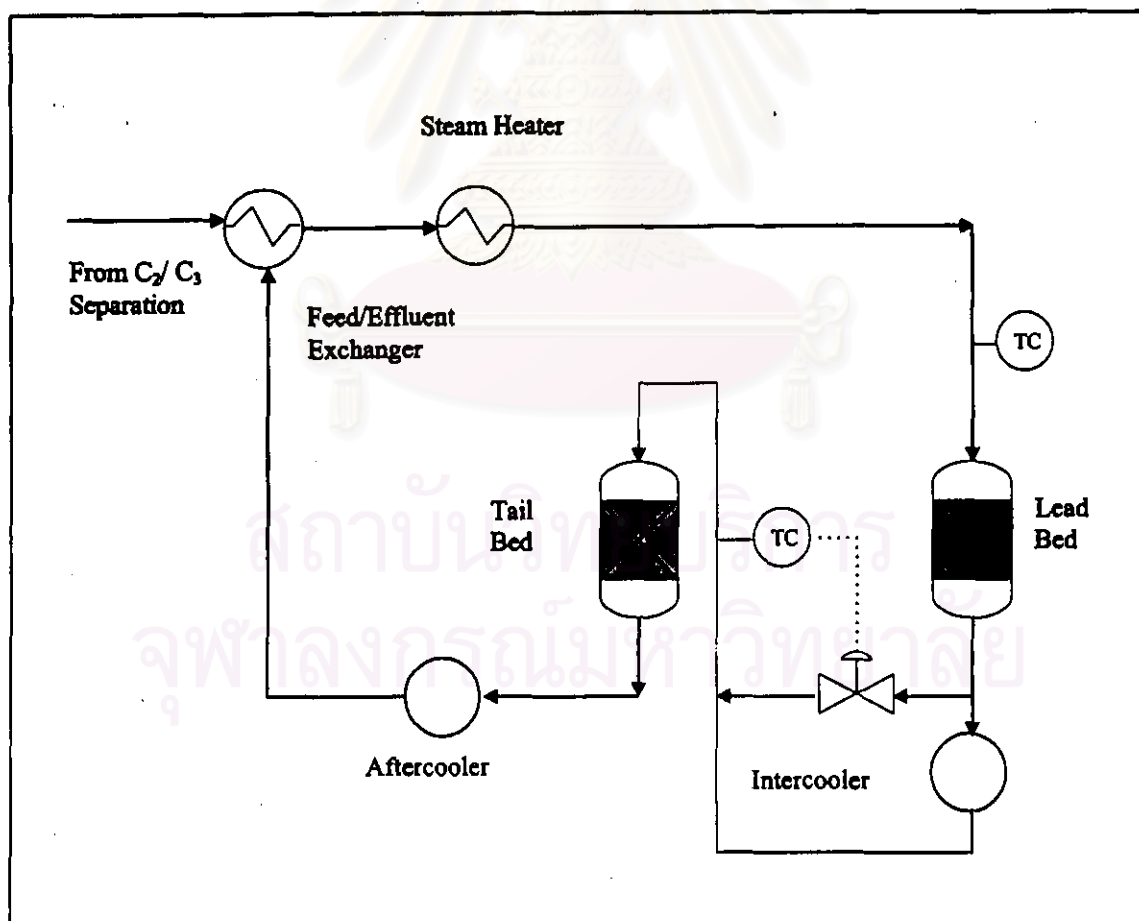


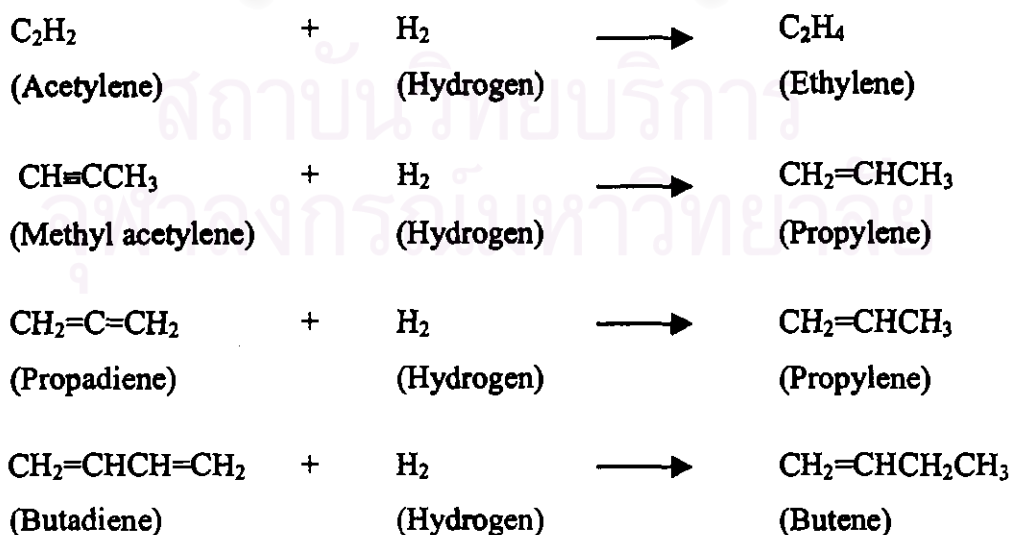
Figure 5.2: Front-end acetylene hydrogenation system layout.

5.3.1 Front-end Type

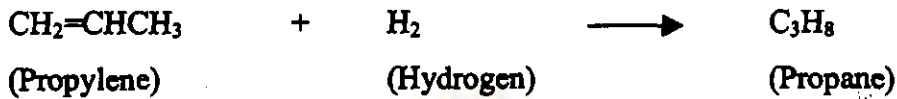
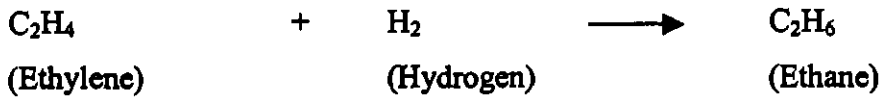
The acetylene hydrogenation system is located prior to the cold train of the ethylene plant (see Figure 5.1). In other words, it is located after the cracking section, following a caustic scrubbing treatment to eliminate carbon dioxide (CO₂). This means that only the inlet temperatures are available as control variables as the cracked gas already contains significant quantities of hydrogen. This option, known as front-end hydrogenation, is the subject of the present work. The industrial sequence under study consists of a heater followed by three fixed-bed adiabatic reactors with interstage cooling. In this unit, the hydrogenation of acetylene is performed directly in the raw cracked-gas mixture, which contains a high H₂/C₂H₂ ratio ($\approx 100/1$). Several acetylenic, olefin and diolefinic by-products are also presented, together with the carbon monoxide (CO) produced in the inverse water-gas shift reaction occurring in the cracking furnaces. The CO is reported to be the main inhibitor of the side C₂H₂ hydrogenation. In practice, these units present important control problems, which frequently lead to undesirable temperature runaways and the subsequent plant shut-down. Figure 5.2 depicts the layout of the front-end acetylene hydrogenation system.

The kinetic reactions occurring in the front-end reactor can be summarized as:

(1) The desired reactions are:



(2) The undesired reactions are:

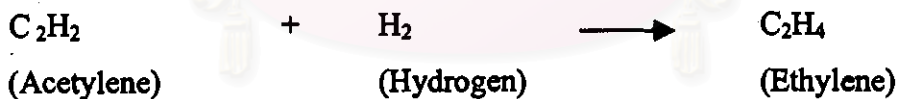


5.3.2 Tail-end Type

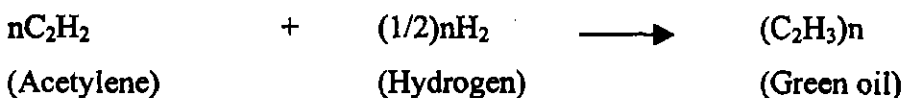
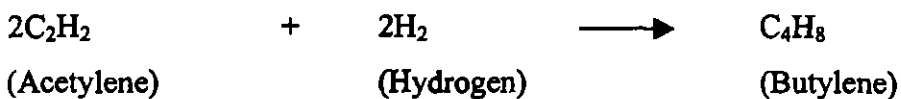
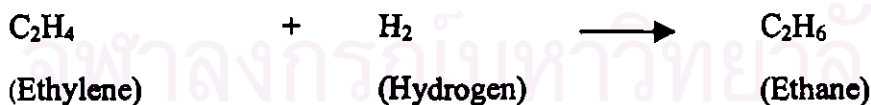
The acetylene hydrogenation system is located after the cold-train (see Figure 5.3) where hydrogen is removed from the cracked gas. That is the system hydrogenates the ethylene-rich stream arising from the top of the de-ethanizer column. Hydrogen must be injected into the feed to the converters and the hydrogen concentration is available as a control variable, in addition to the inlet temperatures to the reactor beds. Figure 5.4 shows the layout of the tail-end acetylene hydrogenation system.

The kinetic reactions occurring in the tail-end reactors can be summarized as:

(1) The desired reaction is:



(2) The side reactions are:



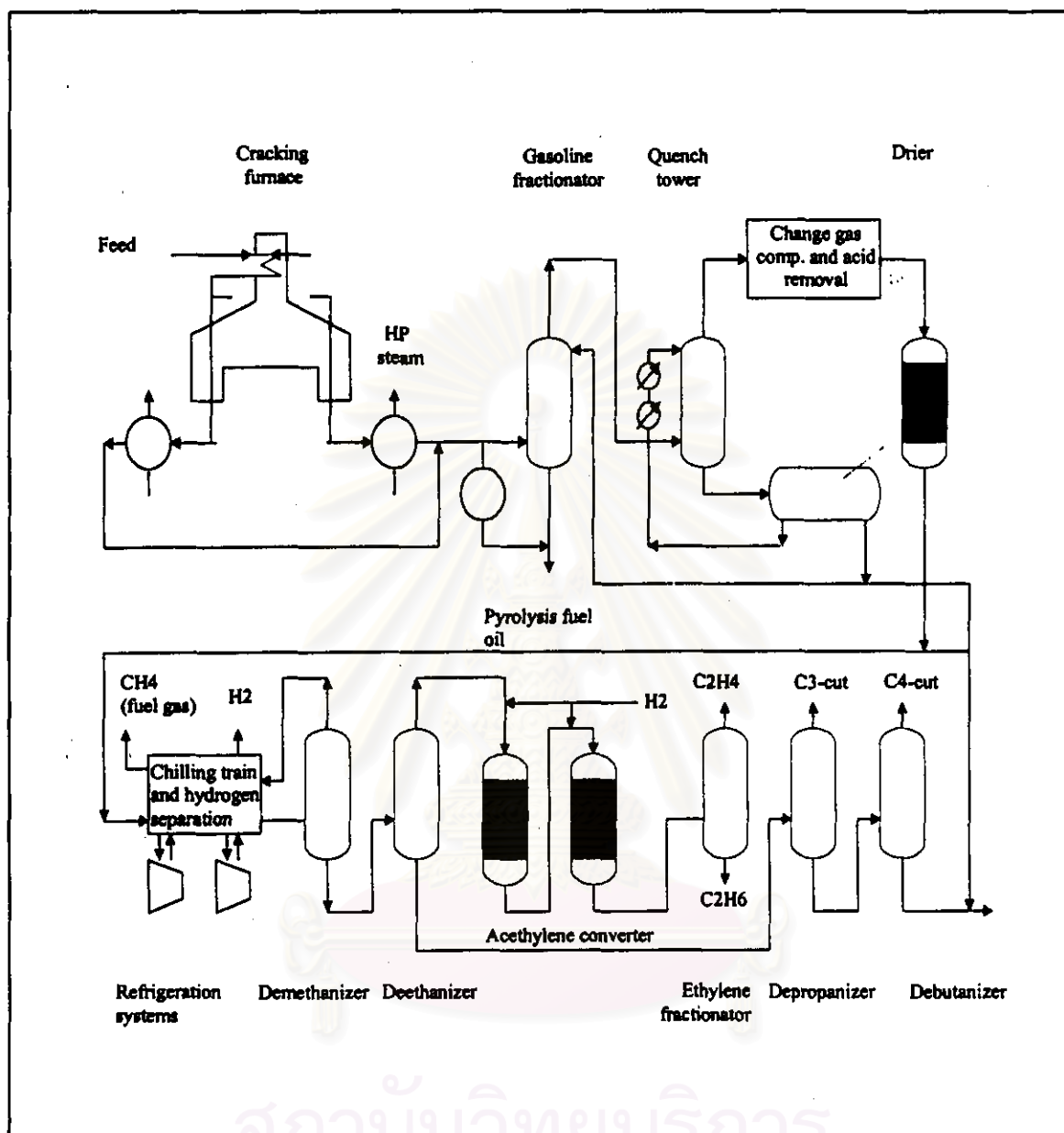


Figure 5.3: Ethylene plant diagram with tail-end acetylene hydrogenation system.

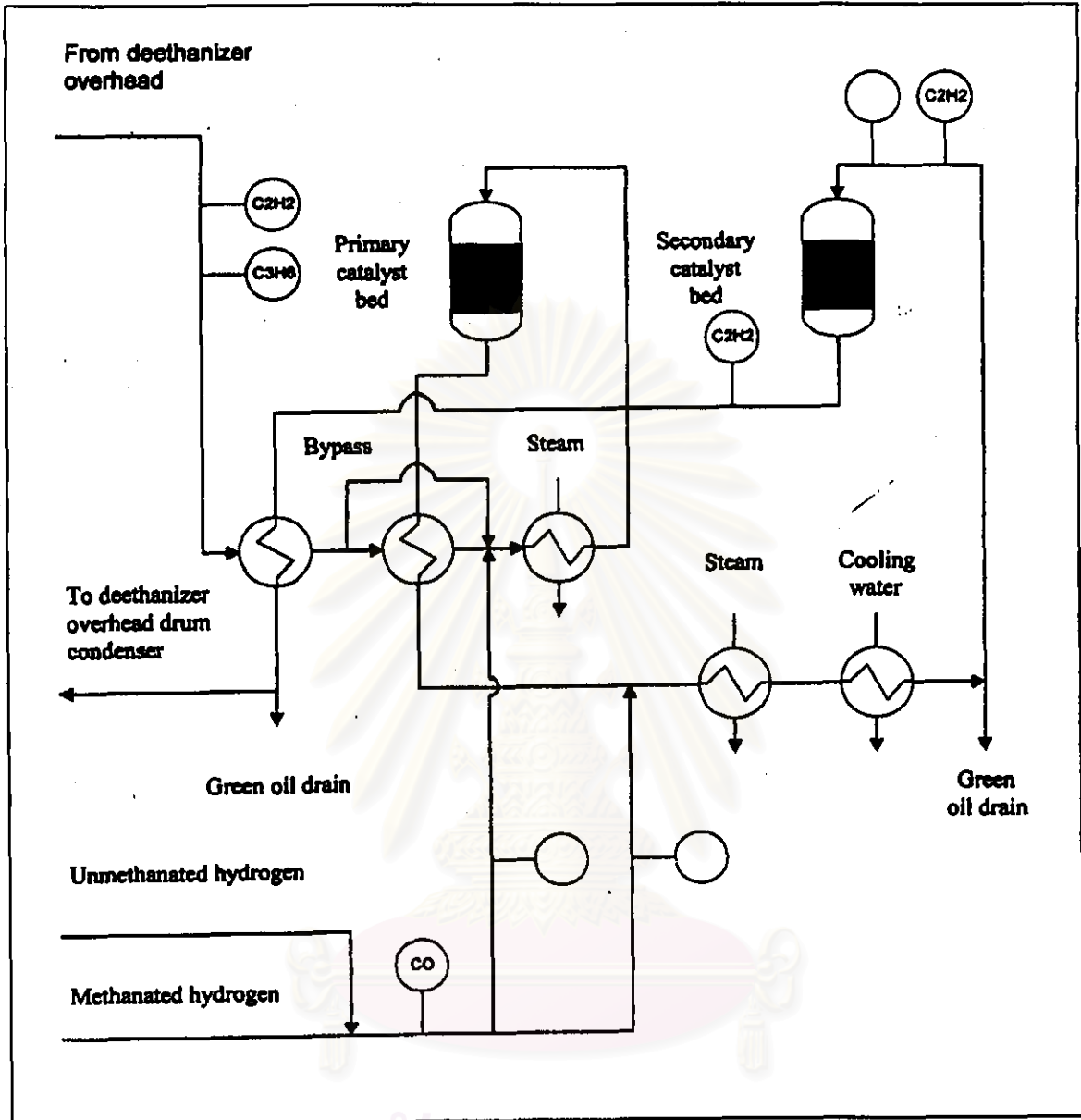


Figure 5.4: Tail-end acetylene hydrogenation system layout.

5.4 Literature Review on Acetylene Hydrogenation Systems

According to the review of research works concerning on the acetylene hydrogenation system, most of the literatures are documented about the studies on the tail-end type. The study on the sensitivity of the reactor operating conditions has been revealed and an optimization based on a reactor model to minimize the ethylene loss while maintaining the outlet acetylene specification has been performed (Huang, 1979). The conjugate gradient methods was used to perform the minimization and arrive at the set of optimal

operating parameters. In addition a general methodology on establishing advanced control schemes of the acetylene hydrogenation reactors has been published (Näsi, 1985). It has presented issues on the online modeling, control and optimization of reactors in an ethylene plant. Nevertheless, the control policy adopted in such research is based upon a static representation of the acetylene hydrogenation system and does not examine the effects over time of the manipulated variables on the deactivation and thus the catalyst regeneration requirements of the hydrogenation process. Therefore, an optimal and a sub-optimal operational policy which minimize the ethylene loss overtime have been formulated and the solution techniques have been presented (Brown, 1991).

However, there are few studies investigating the front-end type. Dynamic simulations of a frontal industrial acetylene converter and its closed-loop performance under three different control strategies have been shown (Schbib et al., 1994). The studies carried out on a mathematical model derived from fundamental equations and checked against industrial data. Moreover, there is other work (Weiss, 1996) studied on the modeling and control of an acetylene converter. It demonstrated that a non-linear dynamic model of process can assist in the development of linear models suitable for controller design. It was also shown that for an industrial acetylene converter, a model based controller should be considered for the control of the reactor outlet temperature.

5.4 Neural Network Modeling of an Acetylene Hydrogenation System

This research studies on the use of multilayer feedforward network to model the front-end acetylene hydrogenation system, thus only the front-end type is concentrated in this section. In order to provide a clearer of the reactor operation, the process description is described. In addition, the plant data used in the research are also provided.

5.5.1 Process Description

Figure 5.5 shows a schematic of the front-end acetylene hydrogenation system used in this research. For producing 385,000 MTA of ethylene, three operating reactors and one

spare are to be utilized. The process sequence consists of three fixed-bed adiabatic reactors with interstage cooling.

The normal acetylene content in the converter feed is 0.3 to 0.5 mol% and the ethylene product acetylene specification is 1 ppmv. The feed to the converter (few C_3 , C_2 and lighter, and CO) comes from the mercury and arsine removal unit which is located after the caustic scrubbing. Mercury and arsine must be removed from the cracked gas because they are poisoned to the palladium catalyst used for selective acetylene hydrogenation. Depending on the catalyst activity, the clean cracked gas flows through or bypasses the reactor feed heater before entering the first reactor. Heat of reaction from acetylene hydrogenation reactors is removed by cooling water in the C_2 hydrogenation intercoolers. The effluent from the third reactor is cooled in the reactor aftercooler.

5.5.2 Plant Data Used

This research is received the cooperation from the Thai Olefin Plant located at Map Ta Phut industrial estate, Rayong province, hence its plant data are used in the research work.

The input-output data of the acetylene hydrogenation system consisting of three catalytic beds in real ethylene plant are collected. The input data of the first bed are composed of cracked gas compositions such as: that of acetylene (C_2H_2), ethylene (C_2H_4), ethane (C_2H_6) and carbon monoxide together with the feed flow rate (F_{in}) and inlet temperature (T_{in}). The output data of the first bed consist of the composition of the acetylene (C_2H_2), that of the ethylene (C_2H_4), that of the ethane (C_2H_6) and the outlet temperature. For the input-output data of the second and the third bed, they are the same as those of the first bed output data except that the inlet temperature of the second and the third bed are used instead of the outlet temperature from the first and the second bed, respectively. However, the collected data need to be filtered before they are utilized for neural network modeling. More details about the filters are given in Appendix C.

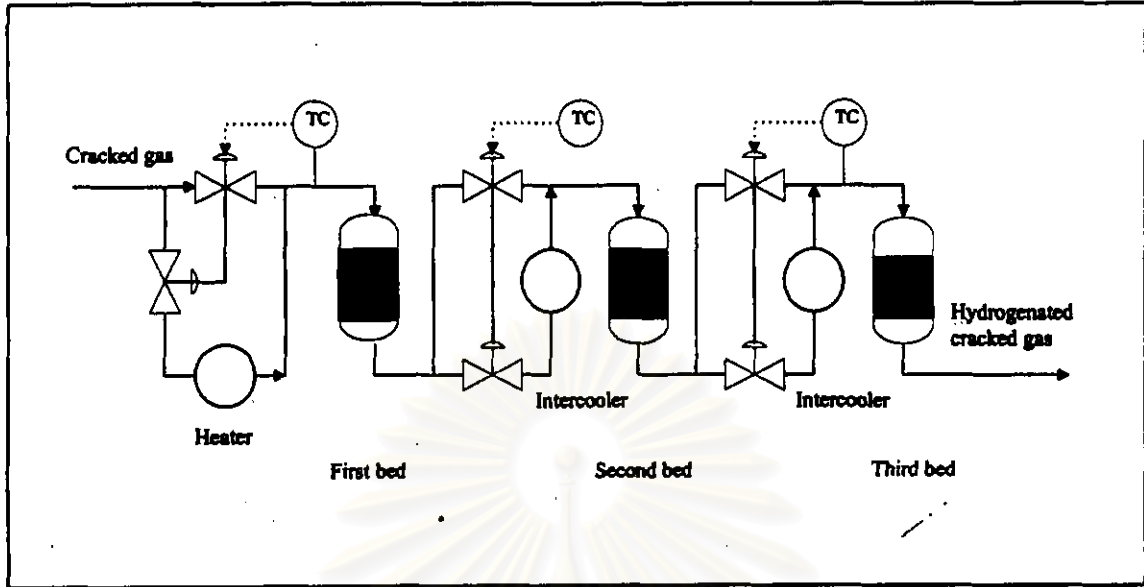


Figure 5.5: Acetylene hydrogenation system.

5.5.3 Neural Network Modeling

In this work the multilayer feedforward networks with one hidden layer are utilized to model the behaviors of the front-end acetylene hydrogenation system. Due to the system consisting of three beds in series, the neural network modeling technique is applied to model the behavior of each bed. Error backpropagation algorithm is used to train the networks. The input-output daily data in amount of 317 data points were used for neural network training and cross validation. That is 290 data points were used for training and the remains were employed for cross validation. The training iteration was set to 1000. Note that one iteration involves application of all the 290 patterns in the training set.

The input vector used for neural network modeling of each bed is composed of the current and one past value of each input and one past value of each output. Each neural network model obtained is applied to predict four outputs. The numbers of hidden nodes in the selected neural network model of the first, the second, and the third bed is 11, 7, and 13. The neural network structure for forward modeling of the first bed is shown in Figure 5.6. The prediction results of the trained network in training and testing data sets are demonstrated in Figure 5.7 and Figure 5.8. For those of the second and the third bed modeling, they are illustrated in Figure 5.9 to Figure 5.11 and Figure 5.12 to Figure 5.14, respectively.

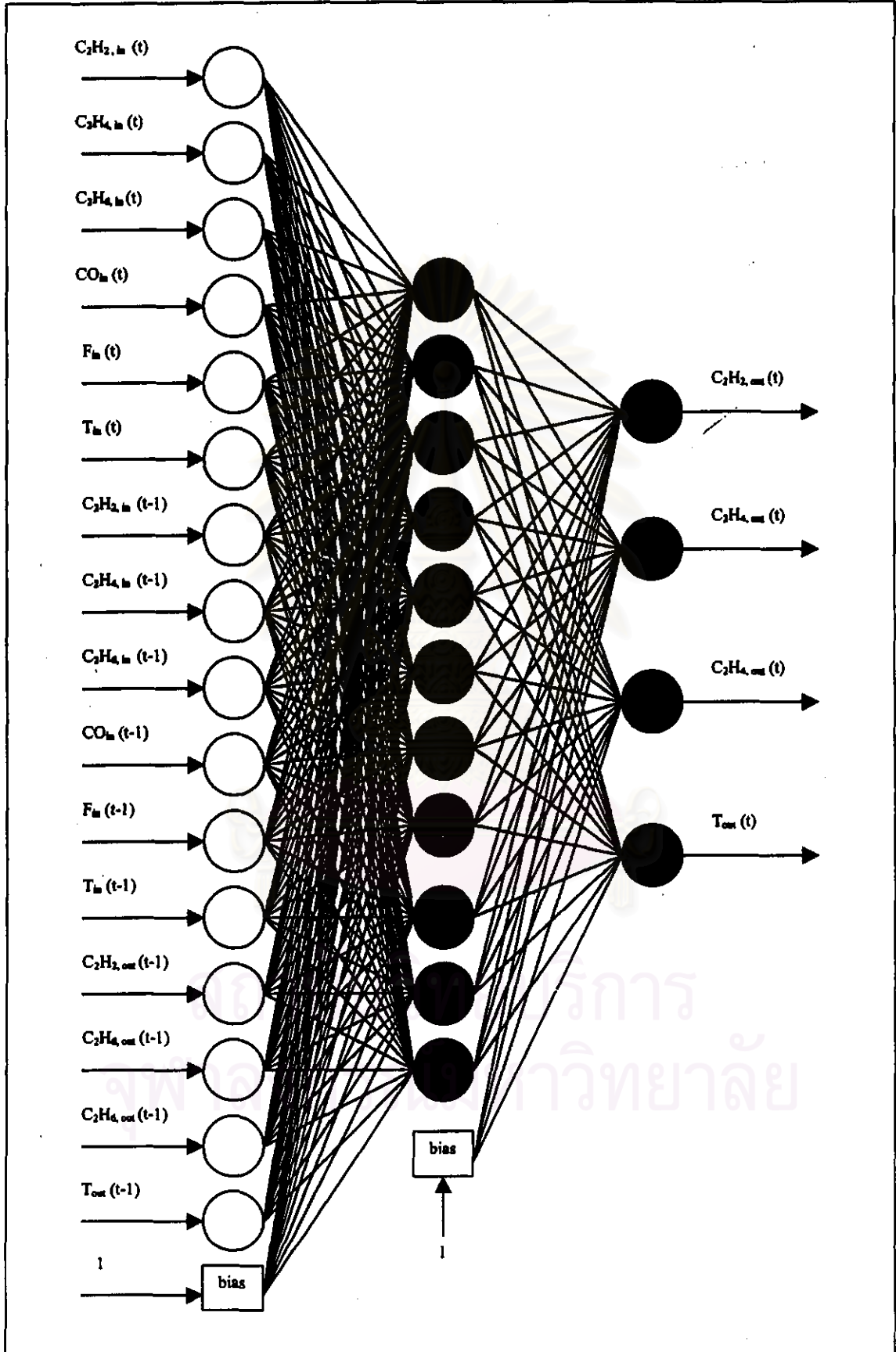


Figure 5.6: Neural network architecture representing forward model: First bed.

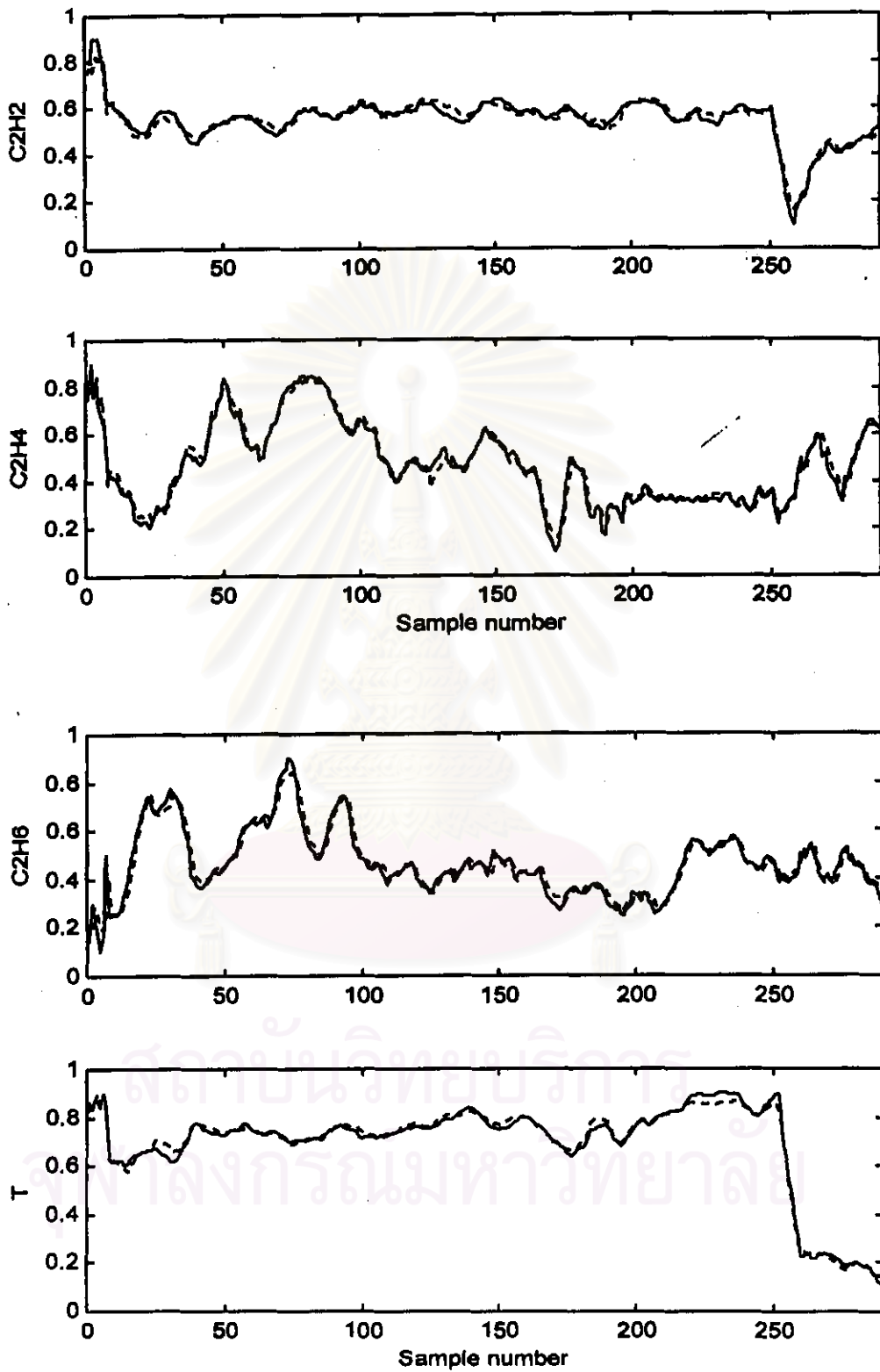


Figure 5.7: Neural network modeling of the first bed: Training results.
Targets (solid line) and NN predicted outputs (dashed line)

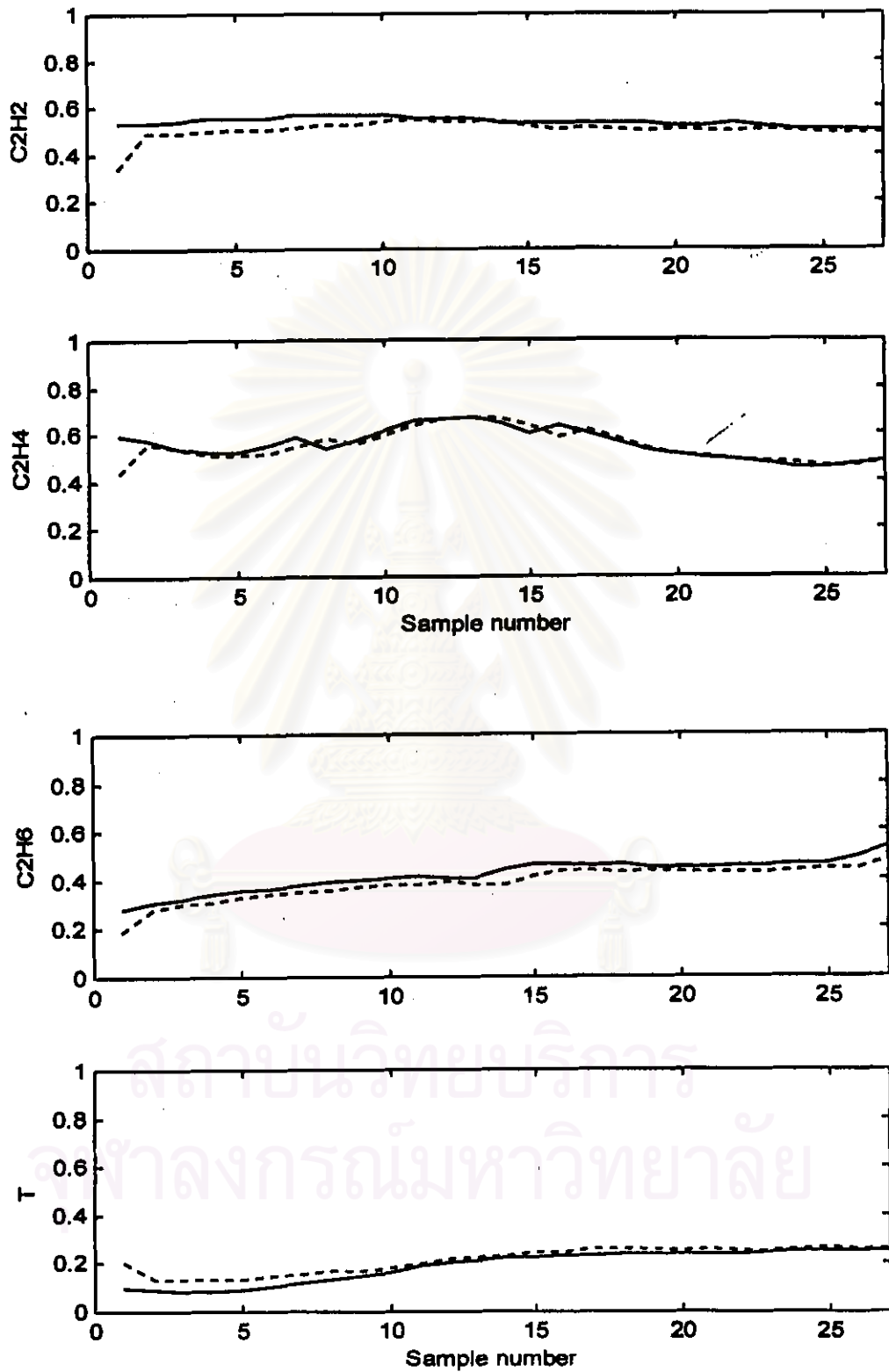


Figure 5.8: Neural network modeling of the first bed: Testing results.

Targets (solid line) and NN predicted outputs (dashed line)

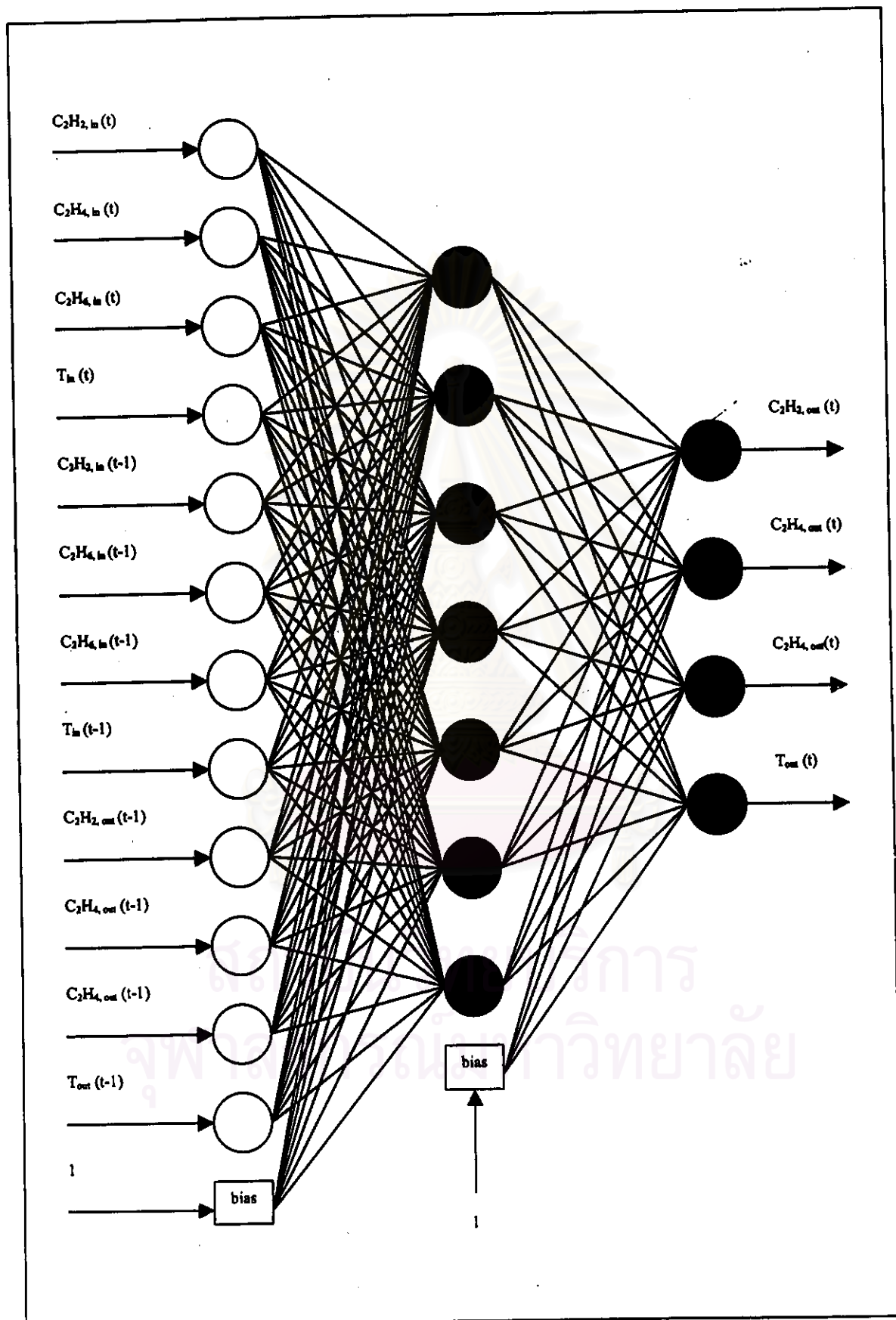


Figure 5.9: Neural network representing forward model: Second bed.

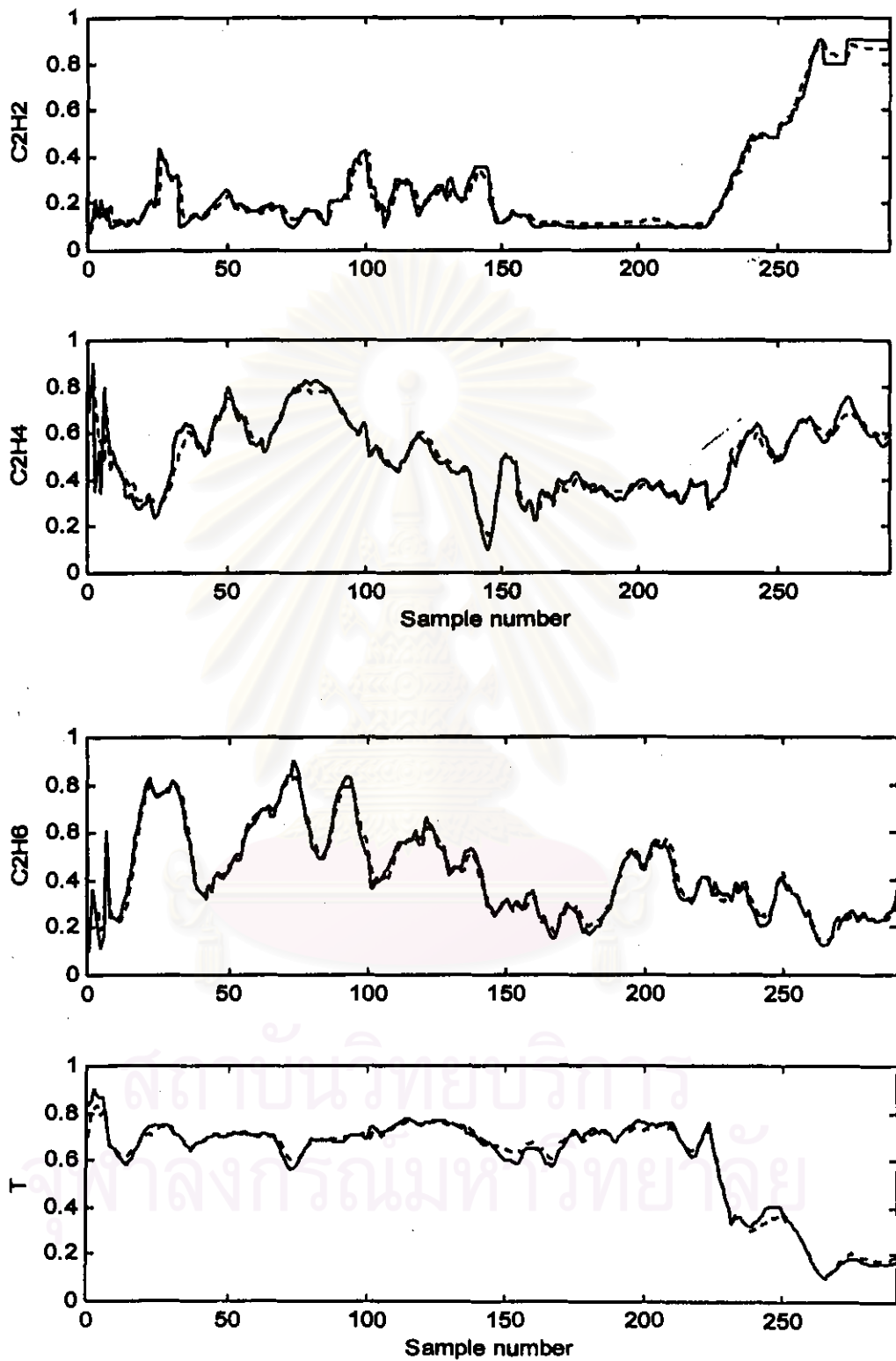


Figure 5.10: Neural network modeling of the second bed: Training results.
Targets (solid line) and NN predicted outputs (dashed line)

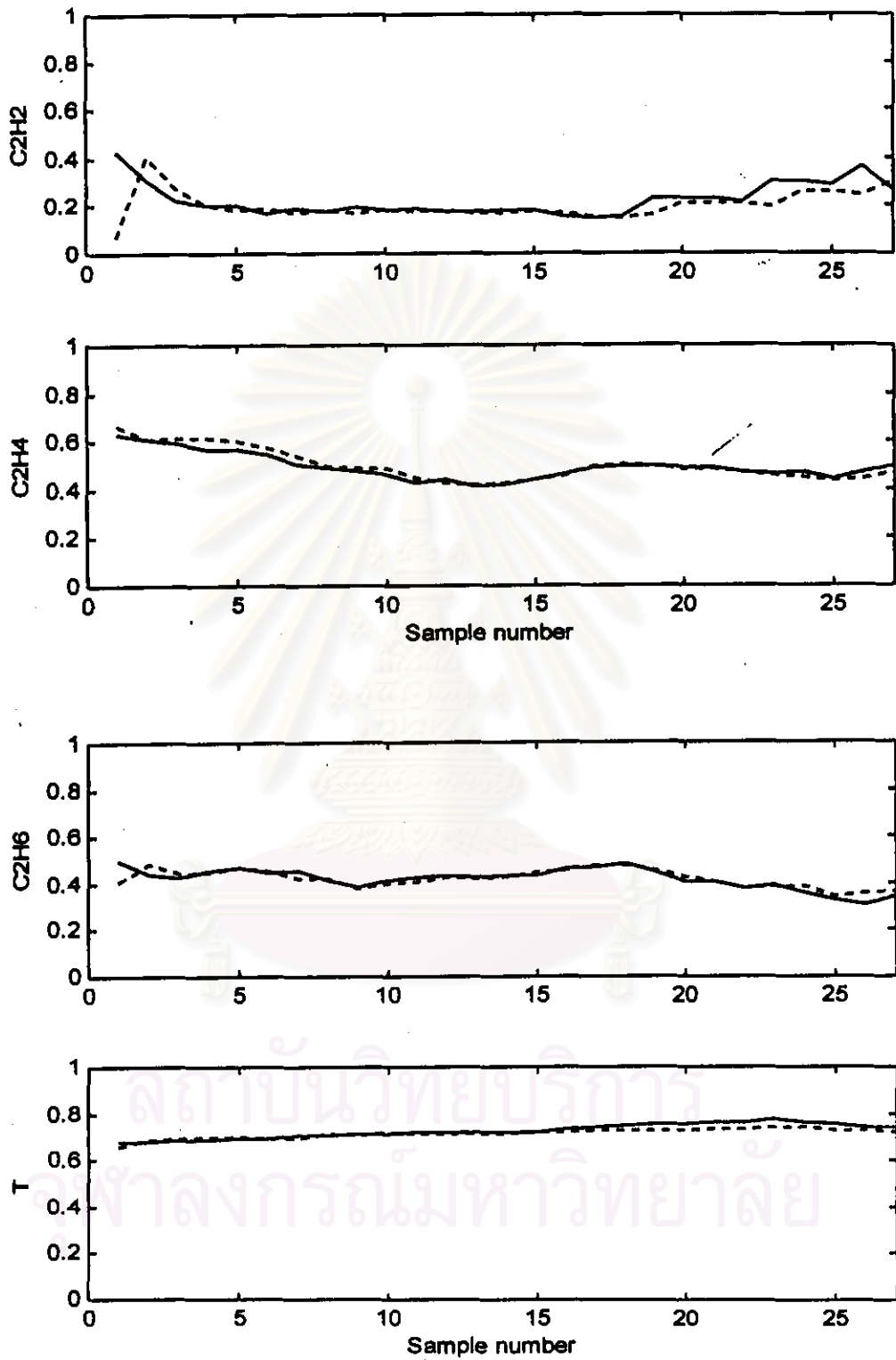


Figure 5.11: Neural network modeling of the second bed: Testing results.
Targets (solid line) and NN predicted outputs (dashed line)

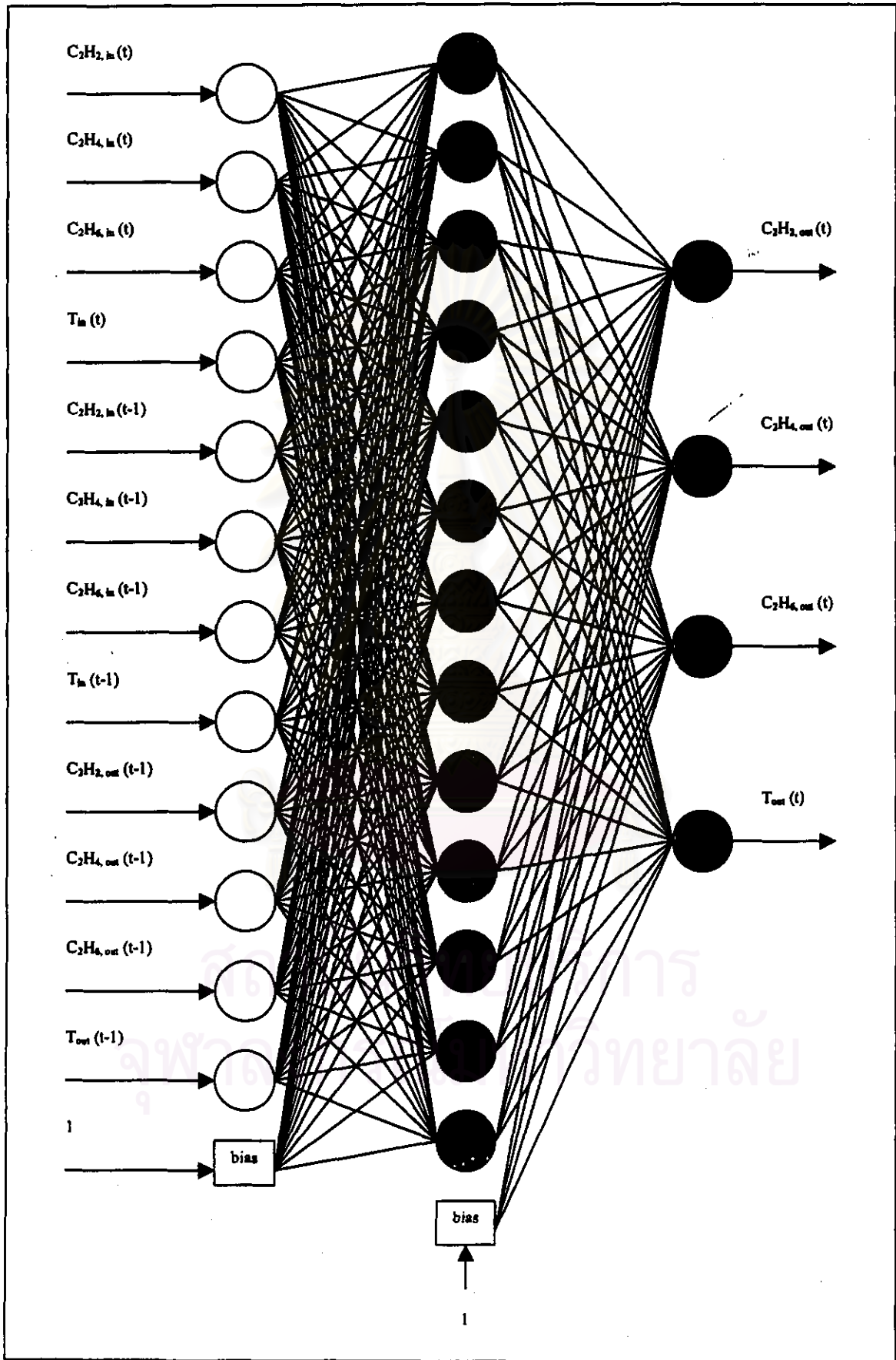


Figure 5.12: Neural network representing forward model: Third bed.

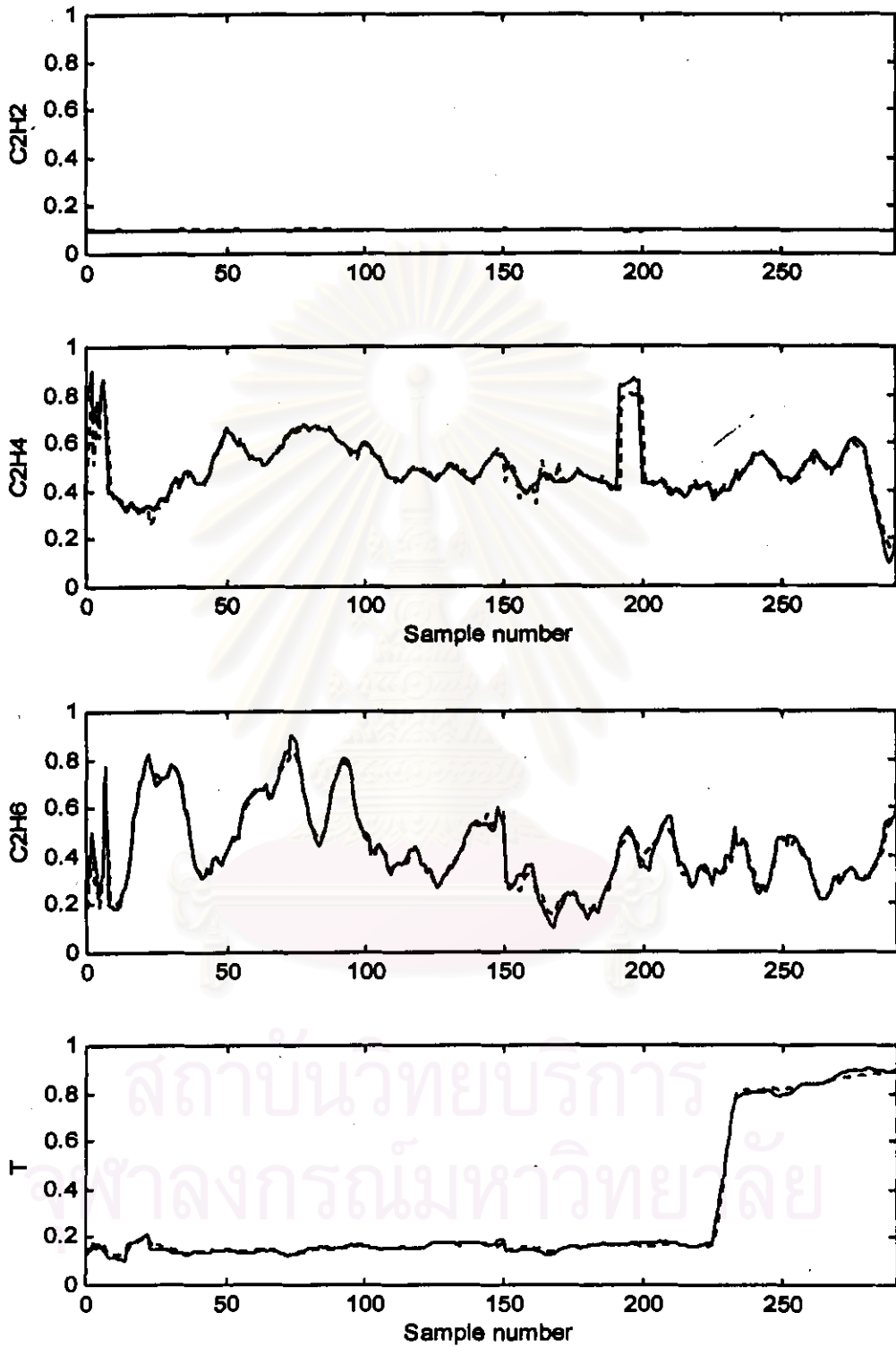


Figure 5.13: Neural network modeling of the third bed: Training results.
Targets (solid line) and NN predicted outputs (dashed line)

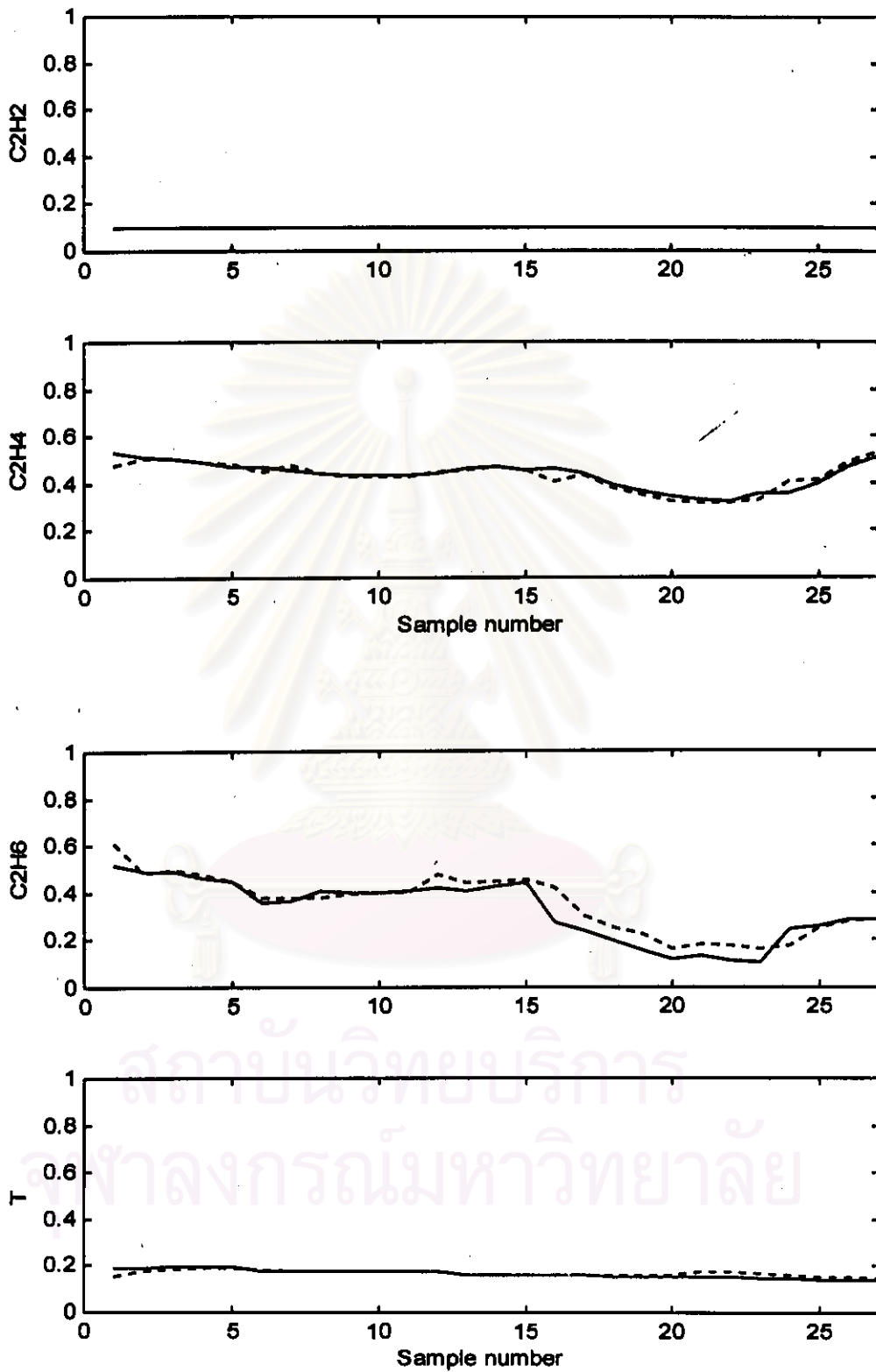


Figure 5.14: Neural network modeling of the third bed: Testing results.
Targets (solid line) and NN predicted outputs (dashed line)

5.5.4 Results and Discussions

According to the first bed modeling, it was found that the prediction of four outputs: the composition of acetylene, the composition of ethylene, the composition of ethane and outlet temperature in the training (Figure 5.7) is quite good especially for the prediction of the last one. However, some errors exist at the initial point of the prediction due to the lack of the past values of input and output data as shown in Figure 5.8.

For the results obtained from the second bed (Figure 5.10 to Figure 5.11) and the last bed modeling (Figure 5.13 to Figure 5.14), they seem similar to those of the first one. In addition to the third one, the prediction of the acetylene composition, which is a constant, is really workable in both training and cross validation. This is probably caused from the neural networks, which are able to learn linear to highly nonlinear relationship. Furthermore, the prediction results of the outlet temperature of the every bed are very good compared to those of the other outputs. It may be because the measurement of the temperature is so accurate that neural networks can learn the correct relationship between the inputs and the outlet temperature. And the reason why the prediction of the composition of the three outputs does not occur precisely is that the analysis by the gas chromatography may have produced some errors due to the small amount of each component, which is hard to be analyzed accurately.

So it can be inferred that the neural networks are able to model the complex system with multiple inputs and multiple outputs. Nevertheless, the data used to train the networks should be composed of sufficient information of system behavior and be filtered before employing them for neural network modeling as described in Chapter 4. The average absolute relative errors of each model obtained are given in the table.

Model	Average Absolute Relative Errors (%)			
	C ₂ H ₂	C ₂ H ₄	C ₂ H ₆	T _{out}
First bed	6	4	8	2
Second bed	7	3	4	2
Third bed	1	4	5	4